JACS
JOURNAL OF THE AMERICAN CHEMICAL SOCIETY

COMMUNICATION

pubs.acs.org/JACS

Preparation and Characterization of a Tetrabutylammonium Graphite Intercalation Compound

Weekit Sirisaksoontorn, Adeniyi A. Adenuga, Vincent T. Remcho, and Michael M. Lerner*

Department of Chemistry, Oregon State University, Corvallis, Oregon 97331-4003, United States

Supporting Information

ABSTRACT: The intercalation of tetrabutylammonium (TBA) cations into graphite by cation exchange from a sodium-ethylenediamine graphite intercalation compound yields a single-phase first-stage product, C_{44}TBA, with a gallery expansion of 0.47 nm. The gallery dimension requires an anisotropic "flattened" cation conformation.

Both anions and cations, including their solvated forms, can intercalate between graphene sheets via oxidation or reduction reactions, respectively, forming graphite intercalation compounds (GICs). A variety of applications for GICs have been proposed or realized, including use as gas physiosorbers,[1] battery electrodes,[2] highly conductive materials,[3] and exfoliation precursors.[4] The syntheses, compositions, and properties of a broad range of GICs containing different intercalate species have been studied. There are many practical and potentially scalable methods for synthesizing GICs from graphite involving chemical oxidants or reductants;[5−8] however, there are relatively few reports on the use of ion exchange or displacement reactions to form new GICs.[9]

The report of monolayer graphene by Geim et al. in 2004,[10] has spurred the search for a scalable route to graphene by solution-phase exfoliation of GICs. A likely strategy involves finding methods to intercalate large and low-charge-density ions into graphite. Tetraalkylammonium cations (TAAs) have been used extensively to modify or delaminate layered hosts,[11−14] including expanded graphite sulfate.[15]

The intercalation of TAAs in graphite has been previously described using electrochemical reduction in polar aprotic organic solvents which are stable against cathodic reduction,[16−20] e.g. DMF (*N*,*N*-dimethylformamide), 1,2-dimethoxyethane, dimethylsulfoxide (DMSO), or propylene carbonate. Besenhard et al. reported a first-stage GIC with DMSO-solvated tetramethylammonium (TMA) cations, C_{24}TMA(DMSO)$_6$, with a basal repeat distance of 1.582 nm.[16] The material was dull black and highly air sensitive. Simonet et al. reported the electrochemical intercalation of TAAs in graphite, but did not obtain product structures or compositions.[19] On the basis of on electroanalytical estimates, those GICs were found to exhibit low intercalate contents, e.g. $C_{400-100}NR_4$.

In the following report, we describe a new exchange reaction where TBA cations rapidly displace a sodium-ethylenediamine Na(en)$_y^+$ cationic complex within graphene galleries. The resulting GIC shows increased gallery expansion, and the product composition is determined using thermogravimetric analysis (TGA) and capillary zone electrophoresis (CZE).

Initially, the first-stage GIC was synthesized by combining Na metal (0.050 g) and graphite powder (0.250 g, SP-1 grade, average particle diameter 100 μm) in ethylenediamine (3 mL). The reaction mixture was continuously stirred at 60 °C for 24 h under an inert atmosphere. After separating the supernatant solution by centrifugation, the blue solid product was dried *in vacuo* at room temperature for 12 h. The displacement reaction was subsequently performed by addition of 0.1 M TBA bromide (0.064 g) to C_{15}Na(en)$_{1.0}$ (0.070 g) in DMF (2 mL). The reaction mixture was stirred at 60 °C for 1.5 h under an inert atmosphere. The black solid was separated from the supernatant solution by centrifugation and then dried *in vacuo* at 60 °C for 6 h. The top phase solution was diluted into DI water for CZE analysis (see Supporting Information [SI]).

Powder XRD patterns for the products obtained are shown in Figure 1. C_{15}Na(en)$_{1.0}$ (Figure 1b) exhibits the characteristic pattern of first-stage GICs with a basal repeat distance (I_c) of 0.671 nm. Subtracting the graphene sheet thickness (0.335 nm) gives an expansion (Δd) along the *c*-direction of 0.336 nm due to the intercalation of the Na-en cationic complex. We will later report further details on this GIC structure and composition. After the displacement reaction, the product is transformed into a GIC with I_c = 0.802 nm (Figure 1c), corresponding to a first-stage product with Δd = 0.467 nm.

Scanning electron micrographs (SEM) of graphite, C_{15}Na(en)$_{1.0}$, and C_{44}TBA show the layered morphology retained for both GIC products, with the latter case showing evidence of increased particle delamination and curved edges. (Figure 2)

It is interesting to note that obtained C_{44}TBA does not hydrolyze readily in air, water, or even aqueous acid (see SI). Because of this stability, it was not possible to fully digest C_{44}TBA to graphite in order to obtain sample compositions. Instead, compositions were determined by following TBA displacement of Na(en)$^+$. Figure 3 shows the capillary electropherogram of the top phase solution following the displacement reaction. Three major solute components are separated by migration time; ethylenediamine, Na and TBA. The recoveries of en and Na from the starting GIC are approximately quantitative, 110 and 93%, respectively (variation from 100% likely stems from a variability in starting GIC composition). The depletion of TBA from solution provides a product composition of C_{43}TBA. This closely agrees with thermogravimetric data as indicated below

Received: June 9, 2011
Published: July 22, 2011

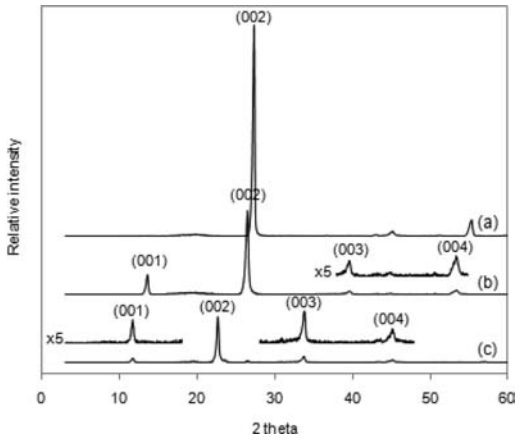

Figure 1. Powder XRD patterns of (a) graphite, (b) $C_{15}Na(en)_{1.0}$ and (c) $C_{44}TBA$.

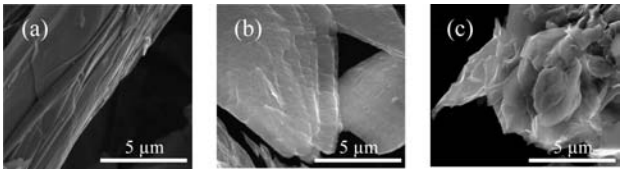

Figure 2. SEM images for (a) graphite, (b) $C_{15}Na(en)_{1.0}$, and (c) $C_{44}TBA$.

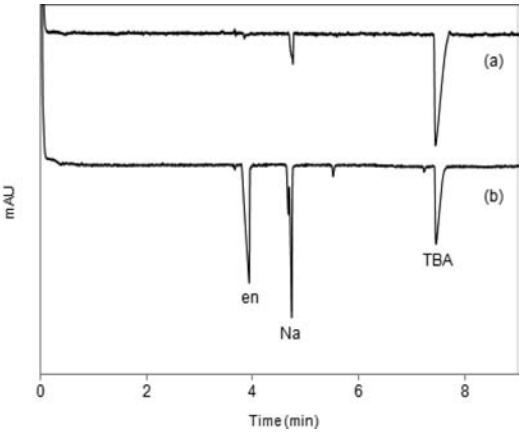

Figure 3. Capillary electropherograms of (a) the TBA solution before displacement and (b) the top phase solution following the displacement of TBA for $Na(en)^+$.

In order to further evaluate GIC compositions, thermal decomposition curves were obtained (Figure 4). Data obtained for graphite and TBA bromide are provided for comparison. $C_{15}Na(en)_{1.0}$ shows a mass loss at 50−150 °C (17.4%) which is attributed to the volatilization of en (Figure 3b). $C_{44}TBA$ (Figure 4c) shows two prominent mass losses at 150−300 °C and 350−500 °C (total loss =31.5%) ascribed to the two-step thermolysis of the TBA intercalate. The two step mass loss has been observed previously for TBA[33] and for GICs with large intercalates.[6] These mass losses yield a product composition of $C_{44}TBA$. Graphite and all GICs begin to lose graphitic carbon mass above 600 °C due to combustion by trace O_2 in the flow gas.

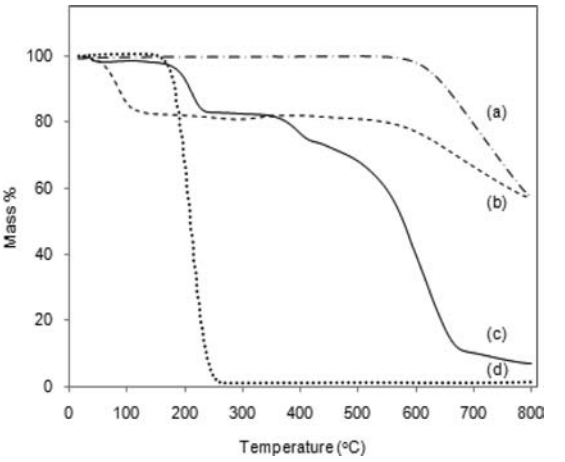

Figure 4. TGA curves of (a) graphite, (b) $C_{15}Na(en)_{1.0}$, (c) $C_{44}TBA$, and (d) TBA bromide salt.

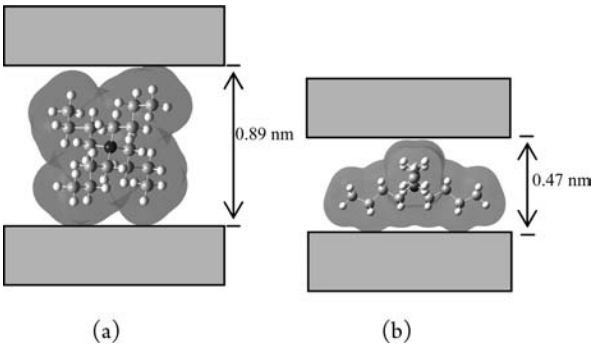

Figure 5. Different TBA conformations inside the graphene layers; (a) fully tetrahedral and (b) flattened. The B3LYP with a 6-31G* basis set was used for energy optimization of the gas-phase cations.

As noted above, the gallery expansion associated with TBA intercalation is 0.467 nm. In clay minerals,[21−24] e.g. montmorillonite, smectite, or in metal oxide/sulfide layered structures,[25−32] e.g. MnO_2, $H_{0.2}RuO_{2.1}\cdot nH_2O$, $Na_2Si_{14}O_{29}\cdot xH_2O$, $H_{0.7}Ti_{1.825}\square_{0.175}O_4\cdot H_2O$, NbS_2, TiS_2, or TaS_2, the intercalation of TBA results a larger expansion in the range of 0.72−0.91 nm. For example, Sasaki et al. showed that TBA intercalates in layered protonic MnO_2 align with C_2 axis normal to the host layers with a gallery expansion 0.84 nm.[11] Considering the crystallographic ionic diameter of TBA (≈0.99 nm),[31] an expansion of >0.8 nm requires only some nestling of intercalate into host sheet surfaces or minor distortion of the TBA conformation.

However, there are some previous reports of TBA intercalation with expansions comparable to that observed for $C_{44}TBA$. Akçay reported a gallery expansion in montmorillonite of 0.49 nm,[33] and Golub et al. found that TBA uptake into MoS_2 under acidic conditions resulted in Δd = 0.52 nm.[34] Figure 5 compares an energy-minimized TBA conformation retaining high symmetry, and requiring a gallery expansion of ≈0.8−0.9 nm (a), and a lower-symmetry conformation requiring an expansion of only ≈0.4 nm. Gas-phase ion energy calculations show a relatively small difference for these conformations (<5 kJ/mol), in agreement with Luzhkov et al. who report a 3 kJ/mol difference for symmetric vs distorted TBA conformations.[35] These conformation energy differences can be offset by a greater lattice enthalpy

associated with smaller lattice expansion. Two factors may tip the energetics in favor of less expansion for TBA in graphite, (1) the delocalization of charge density on graphene sheets, and (2) van der Waals interactions between the graphene sheets and nonpolar intercalates.

The displacement method can be employed to prepare other new C_xNR_4 compounds. Using a displacing tetraoctylammonium (TOA) cation and similar procedures albeit longer reaction time, we have obtained a second-stage C_xTOA (see SI). The gallery expansion is 0.44 nm, indicating that a flattened cation conformation is also adopted for TOA cations.

In summary, we report that tetraalkylammonium ions can be introduced into graphite galleries by a simple displacement reaction. The first stage C_{44}TBA obtained is hydrolytically stable. The gallery expansion of 0.467 nm requires a flattened TBA conformation. Similar reactions with other tetraalkylammonium ions are being explored, preliminary data indicates that TOA also intercalates by this method.

■ ASSOCIATED CONTENT

Supporting Information. Details of the characterization methods for PXRD, TGA and CZE, including the additional results of PXRD for TOA-GIC. This information is available free of charge via the Internet at http://pubs.acs.org.

■ AUTHOR INFORMATION

Corresponding Author
michael.lerner@oregonstate.edu

■ REFERENCES

(1) Purewal, J. J.; Keith, J. B.; Ahn, C. C.; Fultz, B.; Brown, C. M.; Tyagi, M. *Phys. Rev. B.* **2009**, *79*, 054305.
(2) Watanabe, N. *J. Fluorine Chem.* **1983**, *22*, 205–230.
(3) Tsukamoto, J.; Matsumura, K.; Takahashi, T.; Sakoda, K. *Synth. Met.* **1986**, *131*, 255–264.
(4) Malik, S.; Vijayaraghavan, A.; Erni, R.; Ariga, K.; Khalakhan, I.; Hill, J. P. *Nanoscale* **2010**, *2*, 2139–2143.
(5) Özmen-Monkul, B.; Lerner, M. M.; Hagiwara, R. *J. Fluorine Chem.* **2009**, *130*, 581–585.
(6) Maluangnont, T.; Bui, G. T.; Huntington, B. A.; Lerner, M. M. *Chem. Mater.* **2011**, *23*, 1091–1095.
(7) Katinonkul, W.; Lener, M. M. *Carbon* **2007**, *45*, 2672–2677.
(8) Vallés, C.; Drummond, C.; Saadaoui, H.; Furtado, C. A.; He, M.; Roubeau, O.; Ortolani, L.; Monthioux, M.; Pénicaud, A. *J. Am. Chem. Soc.* **2008**, *130*, 15802–15804.
(9) Isaev, Y. V.; Lenenko, N. D.; Gumileva, L. V.; Buyanovskaya, A. G.; Novikov, Y. N.; Stumpp, E. *Carbon* **1997**, *35*, 563–566.
(10) Novoselov, K. S.; Geim, A. K.; Morozov, S. V.; Jiang, D.; Zhang, Y.; Dubonos, S. V.; Grigorieva, I. V.; Firsov, A. A. *Science* **2004**, *306*, 666–669.
(11) Omomo, Y.; Sasaki, T.; Wang, L.; Watanabe, M. *J. Am. Chem. Soc.* **2003**, *125*, 3568–3575.
(12) Tamura, K.; Nakazawa, H. *Clays Clay Miner.* **1996**, *44*, 501–505.
(13) Shiguihara, A. L.; Bizeto, M. A.; Constantini, V. R. L. *Colloids Surf. A* **2007**, *295*, 123–129.
(14) Liu, Z.; Wang, Z.; Yang, X.; Ooi, K. *Langmuir* **2002**, *18*, 4926–4932.
(15) Li, X.; Zhang, G.; Bai, X.; Sun, X.; Wang, X.; Wang, E.; Dai, H. *Nat. Nanotechnol.* **2008**, *3*, 538–542.
(16) Besenhard, J. O.; Möhwald, H.; Nickl, J. J. *Carbon* **1980**, *18*, 399–405.
(17) Besenhard, J. O. *Carbon* **1976**, *14*, 111–115.
(18) Besenhard, J. O.; Fritz, H. P. *J. Electroanal. Chem.* **1974**, *53*, 329–333.
(19) Simonet, J.; Lund, H. *J. Electroanal. Chem.* **1977**, *75*, 719–730.
(20) Noel, M.; Santhanam, R. *J. Power Sources* **1995**, *56*, 101–105.
(21) Ogawa, M.; Handa, T.; Kuroda, K.; Kato, C. *Chem. Lett.* **1990**, 71–74.
(22) Chun, Y.; Sheng, G.; Boyd, S. A. *Clays Clay Miner.* **2003**, *52*, 415–420.
(23) Mercier, L.; Detellier, C. *Clays Clay Miner.* **1994**, *42*, 71–76.
(24) Nakayama, M.; Fukuda, M.; Konishi, S.; Tonosaki, T. *J. Mater. Res.* **2006**, *21*, 3152–3160.
(25) Nakayam, M.; Konishi, S.; Tagashira, H.; Oruga, K. *Langmuir* **2005**, *21*, 354–359.
(26) Gao, Q.; Giraldo, O.; Tong, W.; Suib, S. L. *Chem. Mater.* **2001**, *13*, 778–786.
(27) Fukuda, K.; Kato, H.; Sato, J.; Sugimoto, W.; Takasu, Y. *J. Solid State Chem.* **2009**, *182*, 2997–3002.
(28) Sasaki, T.; Watanabe, M. *Mol. Cryst. Liq. Cryst.* **1998**, *311*, 417–422.
(29) Sasaki, T.; Watanabe, M. *J. Am. Chem. Soc.* **1998**, *120*, 4682–4689.
(30) Peng, S.; Gao, Q.; Du, Z.; Shi, J. *Apply Clay Sci.* **2006**, *31*, 229–237.
(31) Rao, B. L. M.; Halbert, T. R. *Mater. Res. Bull.* **1981**, *16*, 919–922.
(32) Kanzaki, Y.; Konuma, M.; Matsumuto, O. *J. Phys. Chem. Solids* **1980**, *41*, 525–529.
(33) Akçay, M. *J. Colloid Interface Sci.* **2006**, *296*, 16–21.
(34) Golub, A. S.; Zubavichus, Y. V.; Yu, L.; Novikov, Y. N.; Danot, M. *Solid State Ionics* **2000**, *128*, 151–160.
(35) Luzhkov, V. B.; Österberg, F.; Acharya, P.; Chattopadhyaya, J.; Åqvist, J. *Phys. Chem. Chem. Phys.* **2002**, *4*, 4640–4647.